Tsunami simulation for the 2011 Great Tohoku earthquake (*Mw*9.0), Japan, using seismic inversion source model and fully nonlinear tsunami model

A. Petukhin, K. Yoshida & K. Miyakoshi
Geo-Research Institute, Japan

K. Irikura
Aichi Institute of Technology, Professor Emeritus, Kyoto University, Japan

SUMMARY:
The question we addressing here is the possibility of evenly good simulation of observed ground motions and tsunami using the same source model. In this case, for prediction both tsunami and strong ground motions we could use the same source modeling technique. Here we used rupture process of the 2011 Tohoku earthquake inverted using long-period (20-200s) strong-ground motion data. Inverted slip distribution shows large elongated asperity with maximum slip of 47m, which is located on the trench side of the fault. For tsunami propagation and inundation we use fully nonlinear Boussinesq water wave model developed by Wei and Kirby (1995). Simulation results fit observed tsunami waveforms in the off-shore area, both direct and reflected-refracted waves, and reproduce inundation data on the coast of the Sendai plain, Fukushima and S.Sanriku. Simulated waveforms in general reproduce high amplitude short period wave overlapped with long period wave observed at off-shore gauges near Sanriku Coast.

Keywords: Great East Japan earthquake, source characterization, nonlinear tsunami simulation

1. INTRODUCTION

On March 11, 2001, M9.0 earthquake has occurred east off the Pacific coast of Tohoku, as a result of thrust faulting on the interface of plate boundary between the Pacific and North American plates. This earthquake generated tsunami of 30-40m high and strong ground motions up to 1000gal and more. This is one of the best geophysically-recorded great earthquakes and due to this numerous source models were generated using teleseismic, GPS, strong ground motion and tsunami data (e.g. Hayes 2011; Ide *et al*., 2011; Ito *et al*., 2011; Lay *et al*., 2011; Satake *et al*., 2011).

The question we addressing here is the possibility of evenly good simulation of observed ground motions and tsunami using the same source model. In this case we could use source modeling techniques, which were developed for the strong-ground motion prediction (e.g. Irikura and Miyake 2010), for the modeling of tsunami sources and prediction of possible tsunamis. A basement of the seismic source modeling is scaling relations between source parameters, e.g. fault area size, asperity area size, slip value from one side, and seismic moment from another side (Somerville *et al*., 1999; Murotani *et al*., 2008). These scaling relations are estimated by generalization of the seismic source inversion results. As the first step, by comparing simulated and observed tsunami waves we will test source inversion technique on example of the 2011 Tohoku earthquake.

2. SOURCE MODEL

Here we used rupture process of the 2011 Tohoku earthquake inverted by the multi-time window linear waveform inversion method using the long-period (20-200s) strong-ground motion data (Yoshida K. *et al*., 2011). Effects of complicated 3D velocity structure in subduction zone (effects of accretion prism and subducting plate) are negligible in this period range. For this reason accurate and

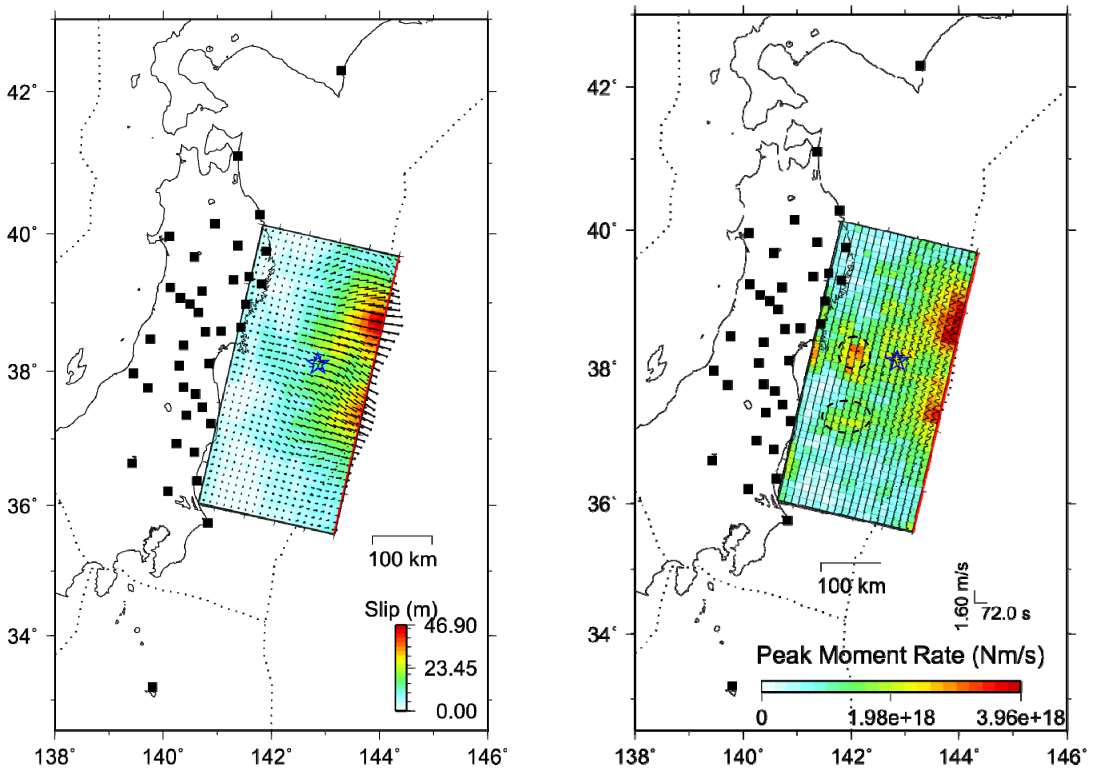

Figure 1. Final slip distribution of the source model of Yosida K. et al. (2011) (left) and distribution of peak moment rate (right). The star and squares indicate the rupture starting point and the strong-motion stations that are used for the inversion. Dotted line shows plate boundaries (Bird, 2003)

computationally effective discrete wavenumber method of Bouchon (1981) combined with 1D propagator matrix algorithm of Kennet and Kerry (1979) can be used for calculation of the Green's functions. From another side, signal-to-noise ratio of 20-200s long-period ground motions is large enough for the *Mw*9.0 earthquake. Velocity records at very hard bedrock sites of the F-net, KiK-net and Hokkaido University seismic networks were used for inversion. A single planar fault model of 475 km in strike and 240 km in dip is assumed based on the 1st day aftershock distribution. The rupture velocity inferred to be slower than 2.5 km/s at early stage of the rupture process. The seismic moment of this earthquake was estimated to be $4.3e10^{22}$ Nm (*Mw* = 9.0).

The inverted slip distribution shows a large elongated asperity (large slip area) with a maximum slip of 47 m which is located on the shallower part of the fault plane, slightly north of epicenter (Fig. 1, left). This is consistent with some other source models (e.g. Ide *et al*., 2011; Lay *et al*., 2011). Areas of the moment rate large amplitudes (shown by dashed line in Fig.1, right), which are responsible for generation of short period ground motions, is shifted to the deeper land-side part of the source and have tendency to scatter in a few strong motion generation areas. This is consistent with the empirical Green's function simulation results of Kurahashi and Irikura (2011). The rupture of these areas radiated short-period components with short pulse width of moment rate functions.

3. TSUNAMI SIMULATION

Numerical simulations of tsunami require three components: (1) source model, reflecting fault location and slip distribution; (2) ocean bathymetry and coastal topography, and (3) tsunami propagation and inundation model.

Seafloor displacement modeled as a sum effect of all seismic subsources of the source model, which are classical dislocation point sources, combining slip motions occurring on the oblique fault plane embedded into semi-infinite elastic medium (Okada, 1985). Shear modulus equal $4.0x10^{10}$ kg/ms^2 is

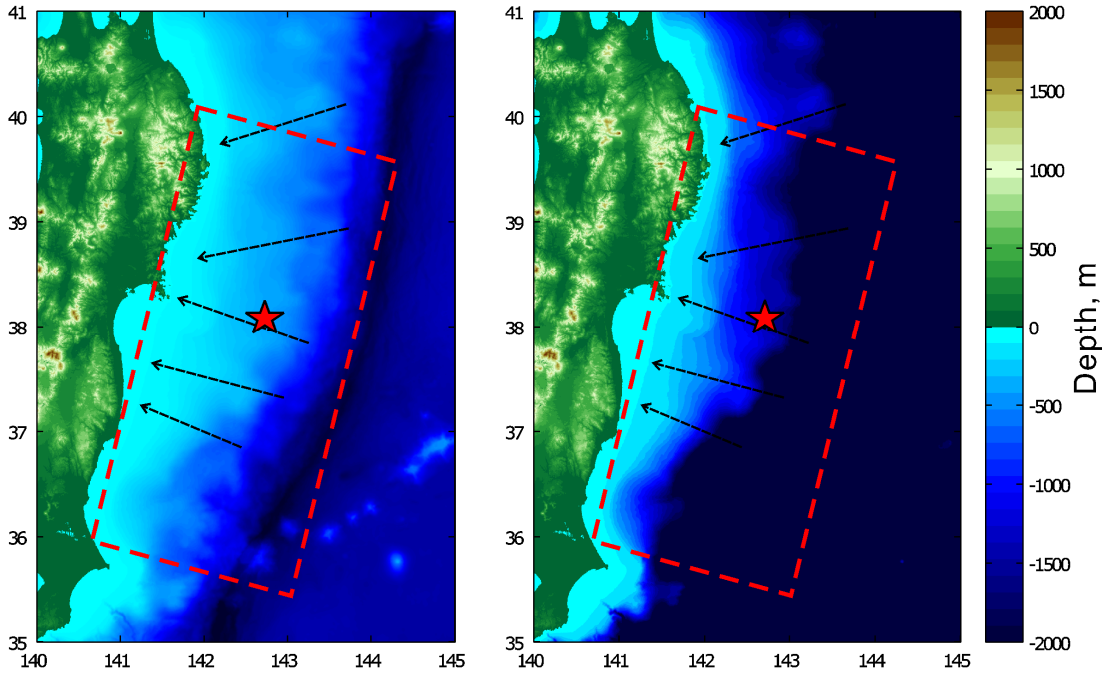

Figure 2. Bathimetry map of the target area. Arrows indicate seafloor ridges, which are potential waveguides of tsunami waves. Red line and star mark indicates source plane and earthquake epicenter. Bathymetry map on the right plot is scaled to 2000m for clarity

assumed. Sea surface elevation is similar to the seafloor elevation. We used time dependent slip rate functions estimated by the multi-time window source inversion on each subfault. We also consider time delay of subsources due to rupture propagation. Although rupture velocity (~2000 m/s) is much higher than tsunami wave velocity (~500 m/s for deep water around the trench), weak effect of tsunami delay due to rupture propagation, which is especially noticeable for short period tsunami wave observed in the Tohoku tsunami, is possible.

Model of ocean bathymetry and coastal topography is compiled from the digital bathymetry map M7000, having resolution less than 50m, from the Japan Hydrographic Association's (JHA) for coastal area, multi narrow beam data from the Japan Agency for Marine-Earth Science and Technology (JAMSTEC) for source area, 50m gridded inland topography of the Digital Elevation Model from the Geospatial Information Authority of Japan (GSI), and 500m gridded bathymetric data set J-EGG500 from the Japan Oceanographic Data Center (JODC) for the rest of the area. Bathymetry map is shown in Fig. 2. Bathymetry resolution 500m is enough for tsunami propagation and inundation in the off-shore area and in simple coast-line environment of Sendai plain and Fukushima prefecture in the southern part of the source region. However, in the northern part of source region, the Ria environment on the Sanriku coast is composed from numerous small size bays, many of them have only 1-3km size, which are just one-to-few grids of bathymetry model. Large simulation errors of inundation and run-up are possible here. Another source of the tsunami wave amplification is the propagation of wave along/above a submarine ridge-like structure. Wave velocity become smaller just above the ridge and higher in neighboring valleys. This results in the geometrical focusing effect increasing amplitude of tsunami wave, even in a flat coastal environment. In Fig. 2 potentially dangerous ridges are shown by arrows.

For tsunami propagation and inundation we use a Boussinesq water wave model developed by Wei and Kirby (1995) (program FUNWAVE). The model is fully nonlinear and dispersive, retaining information to all orders in nonlinearity a/h (where a - wave amplitude and h - water depth). Program includes bottom dissipation and wave breaking, without which the wave would artificially amplify at the coast, and allows simulation of the land inundation through a moving shoreline algorithm, which has been fully validated for short-wave shoaling, breaking and run-up. Method has been calibrated to

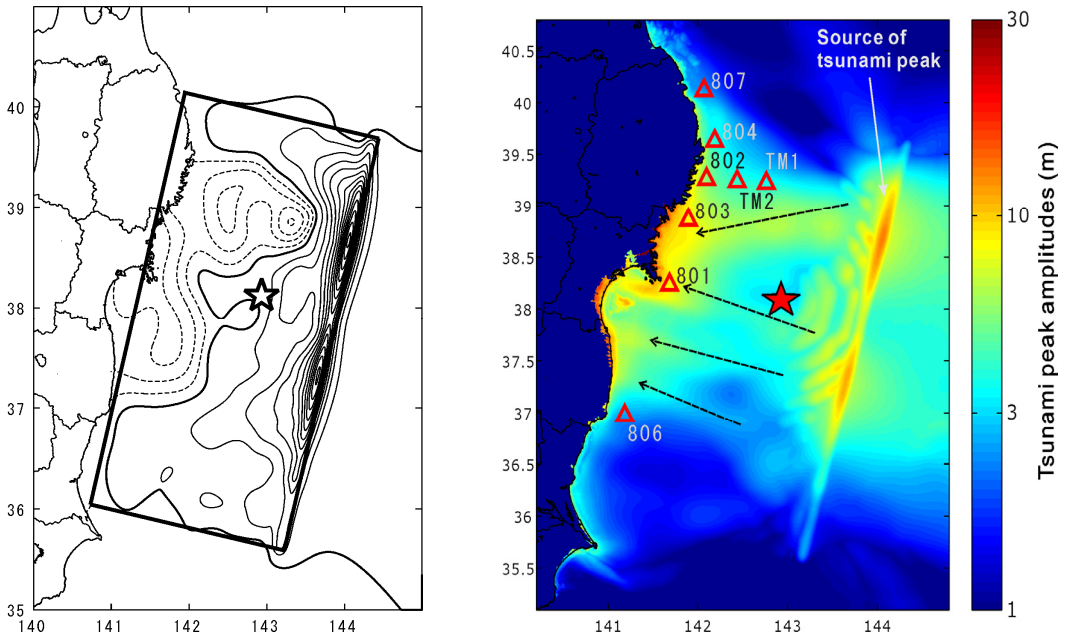

Figure 3. Left: Distribution of the sea surface elevation due to the source slip. Solid contours (1m interval) indicate uplift, dashed contours (0.5m interval) – subsidence, thick contour – zero elevation. Right: Distribution of maximum amplitudes of propagated tsunami waves. Location of the offshore gauges (triangles) and waveguide ridges from Fig. 2 (dashed arrows) are shown for reference.

provide a stable model for tsunami run-up, and has been successfully used to simulate various regional earthquake tsunamis, including devastating 2004 Indian Ocean tsunami (e.g. Ioualalen *et al*., 2006). Simulation area of the 2011 Tohoku tsunami is limited to 140°-145°E and 35°-41°N, for simulation we used 500 m finite difference grid for open ocean area, 150m grid for coastal area of Sendai plain and Fukushima prefecture, and 40m grid for coastal area of Sanriku coast.

4. SIMULATION RESULTS

Results of tsunami simulation are compared with the off-shore gauge waveform data of the Nationwide Ocean Wave Information network for Ports and HArbourS (NOWPHAS, http://nowphas.mlit.go.jp/) and with on shore inundation data of the Tohoku Earthquake Tsunami Survey Group (release 20120228, http://www.coastal.jp/ttjt/). Many coastal tide gauges on the Tohoku coast were broken by the first tsunami wave. Two offshore floating GPS wave gauges number 804 and 802 at a 200m depth (see location in Fig. 3) and two cable pressure-gauges (TM-1 at 1600 m and TM-2 at 1000 m depth) are recorded unusual two-stage tsunamis (Fig. 4). After arrival of a long period tsunami wave, the water level gradually increased up to 2 m during the first 10 min, and then impulsive tsunami wave, having higher amplitude and shorter period of the order 3 min, was observed. There is a tendency that amplitudes of the 20 min long period wave decrease from southern gauge 801 to the northern gauge 807, while amplitudes of the 3min short period wave increase in the same direction.

Due to accurate simulation both open ocean tsunami propagation and land inundation in the fully nonlinear tsunami model, simulation results fit observed tsunami waves in the off-shore area (Fig. 4 left), both direct waves and later reflected/refracted phases. Simulated waveforms in general reproduce two-stage feature of the observed waveforms. We suppose that long period wave is a result of tsunami generation in a wide uplifted area just near and east to epicenter, while the short period wave is a result of high uplift of the ocean surface on the edge of seismic source near the trench (see Fig. 3). This is supported by back projection analysis of tsunami arrival times of Hayashi *et al*. (2011), which show that primary crests of the short period tsunami waves are generated in area centered at point 143.9E/38.5N or even slightly to the North.

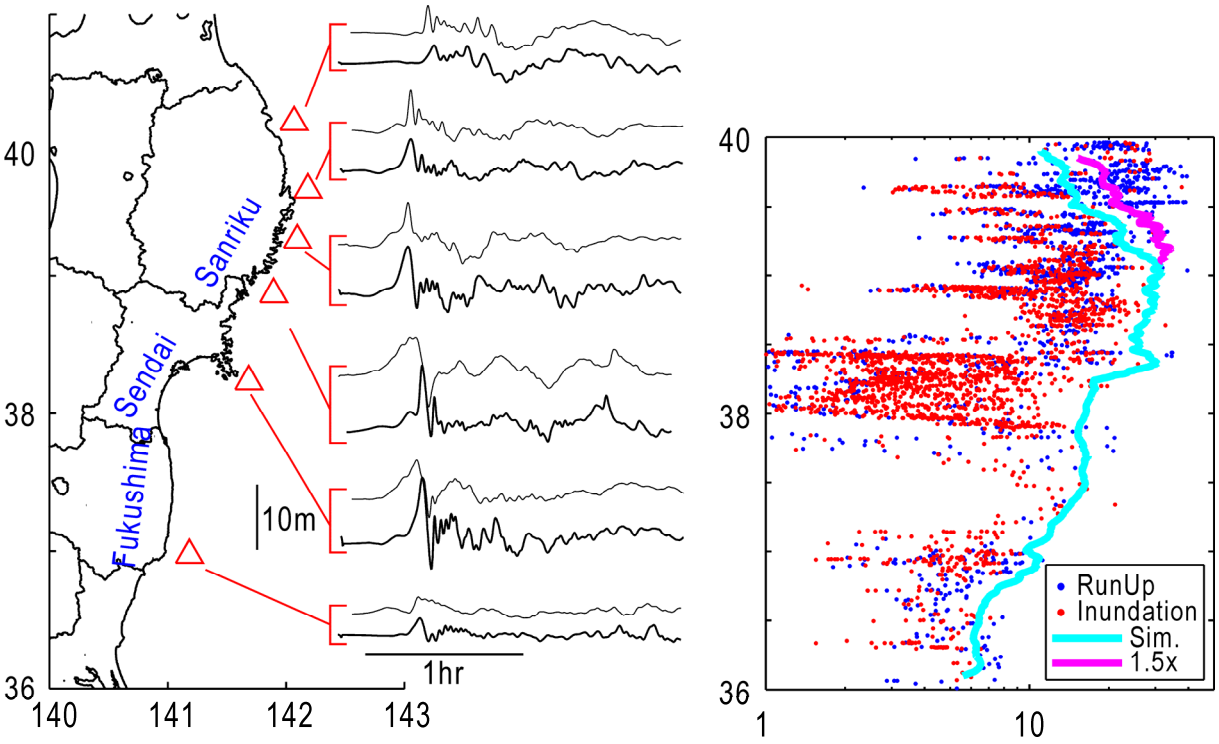

Figure 4. Results for inverted source model. Left: Comparison of observed (upper) and simulated (lower) tsunami waveforms. Right: Comparison of observed run-up/inundation heights (dots) and simulated peak values (line)

Simulation results also reproduce inundation data on the coast of the Sendai plain, Fukushima and South Sanriku (Fig. 4 right). Some variations of the inundation heights are possible both due to effect of waveguides (e.g. Central Fukushima area) and effect of coastal bathymetry (e.g. Northern Miyagi area). On the North Sanriku coast, simulated amplitudes are noticeably smaller than observed ones. We should notice that off-shore amplitudes at the nearest gauge 807 are also underestimated around 1.5 times. We tried to simulate inundation for rescaled input wave too. Results are appended to Fig. 4. They demonstrate that fit of inundation heights become better in this case, but still slightly underestimated. Possible reason of the underestimated simulated amplitudes is a deficiency of the earthquake source modeling, unconsidered additional tsunami sources like submarine landslides or slow-slip events, and/or a small resolution of used bathymetry data for this area.

5. TSUNAMI SIMULATION USING CHARACTERIZED SOURCE MODEL

For prediction of future tsunamis we could try to use characterized source modeling techniques, which were developed for the strong-ground motion prediction (e.g. Irikura and Miyake, 2010). A basement of the seismic source modeling is scaling relations between the characterized source parameters and seismic moment, which are result of generalization of the seismic source inversion results. Here we test source characterization technique for M9 class event on example of the 2011 Tohoku earthquake.

Fig. 5 shows result of characterization of the slip distribution from Fig. 1 using trimming technique of Somerville *et al*. (1999). Bold line indicates asperity. Parameters of the characterized source are shown in Table 1. On Fig. 6 these parameters are compared with the average relationships for subduction zone earthquakes of Murotani *et al*. (2008); good agreement is found.

At the next step we simulated tsunami similarly to the inverted case above. It is natural that pulse width becomes wider in case of characterized source model. For this reason waveform agreement become worth in the northern part (gauges 807, 804 and 802), but much better in the southern part

(gauges 803, 801 and 806, see Fig. 7 left). Contrary, maximum inundation heights distribution didn't change very much (compare Fig. 7 right and Fig. 4 right). Maximum difference is around 40%, which is natural payment for the uncertainty of the source model. We conclude that characterized source approach is promising for tsunami prediction.

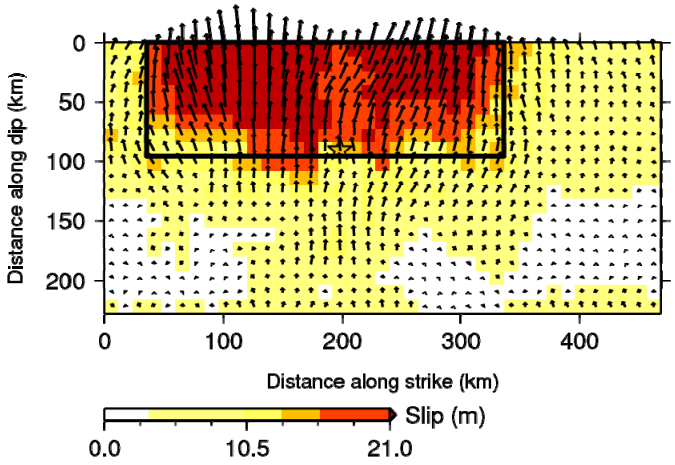

Figure 5. Result of the source model characterization. Thick line indicates characterized asperity.

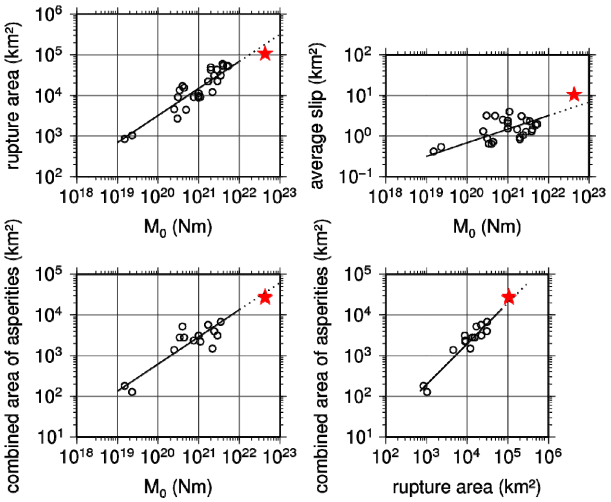

Figure 6. Comparison of parameters of the characterized source model (star) with average relationships (line) for subduction zone earthquakes (circle)

Table 5.1. Parameters of the characterized source model

Source parameter	Value
Total rupture area	1.1281×10^{12} m^2
Combined area of asperities	3.1250×10^{10} m^2
Number of asperities	1
Average slip	10 m
Asperity slip	22 m
Background slip	6 m

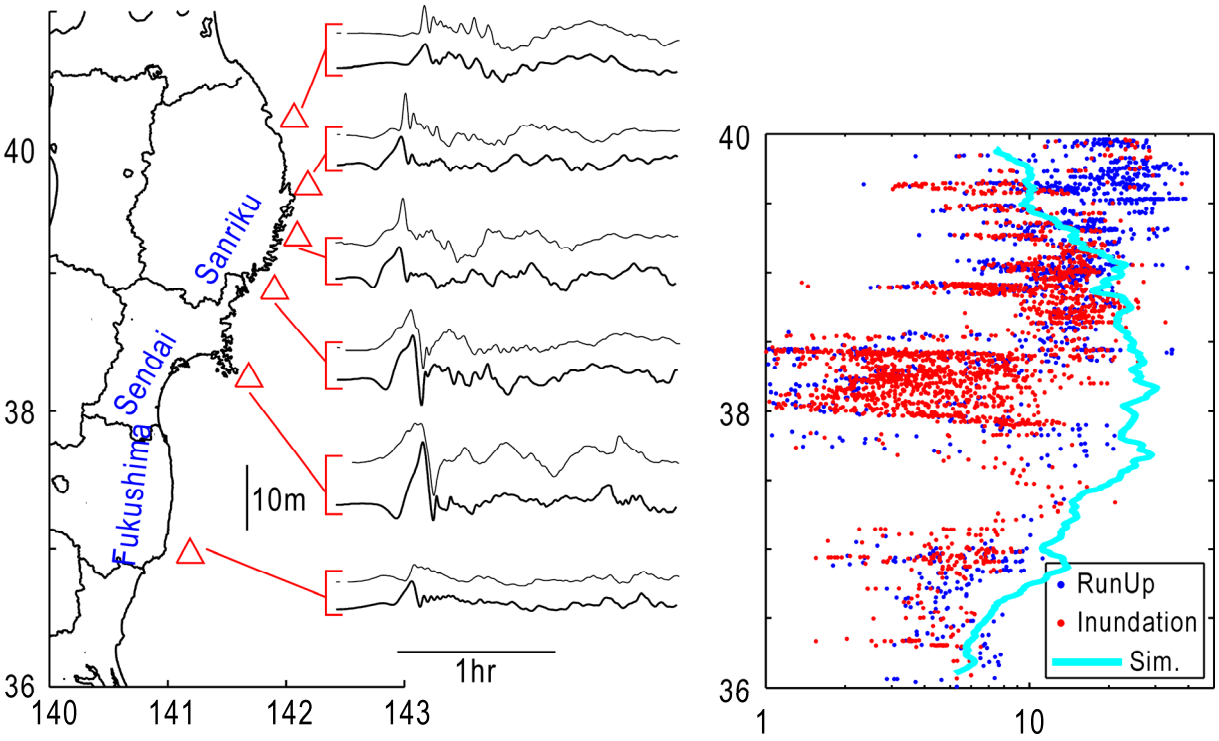

Figure 7. Results for characterized source model. Left: Comparison of observed (upper) and simulated (lower) tsunami waveforms. Right: Comparison of observed run-up/inundation heights (dots) and simulated peak values (line)

6. DISCUSSION AND CONCLUSIONS

Tsunami of the 2011 Tohoku earthquake was simulated using source model estimated by inversion of the long-period strong-motion waveform data. Forward tsunami simulation results demonstrate good agreement with observation data, namely tsunami waveforms for off-shore gauges and on-shore inundation heights. We also verified the characterized source model approach, which is widely used for prediction of the strong ground motions. This indicates that source models developed for prediction of strong ground motions can be used for prediction of tsunami too.

In spite of good fit of tsunami waveforms at off-shore gauges, inundation heights on the North Sanriku coast are underestimated with a factor of 2.5. Due to effect of source, first tsunami wave at the off-shore gauge 807 in this area is underestimated with a factor of 1.5. Inundation heights underestimation, corrected for this underestimation due to source, can be reduced to a factor of 1.7. The fact that off shore tsunami waves are truly simulated, but onshore inundation/run-up heights are underestimated indicates that the reason of the underestimation may be inaccuracy of inundation simulation, for example due to inaccuracy of the bathymetry model. Actually, small scale structures like ridges and canyons on the continental slope, with a few exceptions become unresolved in the most of M7000 bathymetry model area. These small structures may work as amplifiers of the short-length tsunami wave.

Fig. 8 shows example of distribution of observed inundation heights for the Miyako-shi area in North Sanriku. The most striking feature observed here is that high inundations were observed not in narrow conical bays that could be expected from a simplified wave dynamics, but in the cape and cliff areas. This effect maybe possible, if capes are connected with underwater ridges that may work as waveguides and amplifiers of tsunami waves. Further improvements of bathymetry model and additional simulations are necessary to confirm or reject this explanation. Another important effect is the wave splashing, that can increase observed inundation heights but cannot be modeled here.

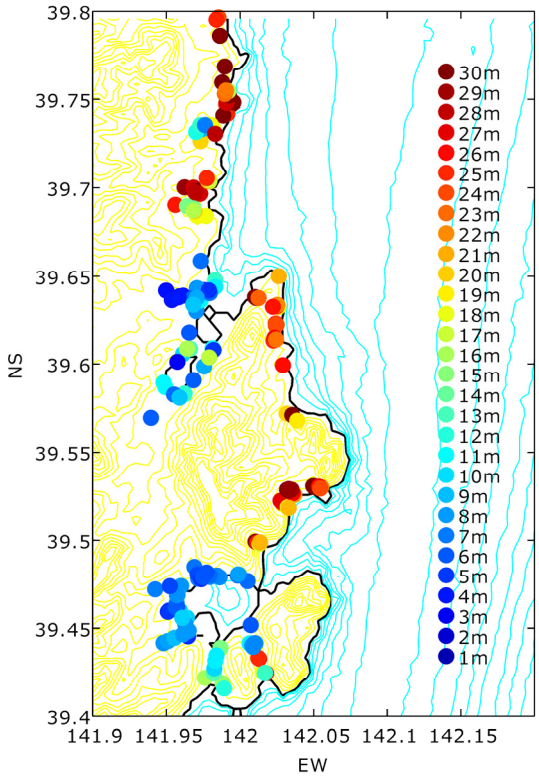

Figure 8. Example of distribution of observed inundation heights for the Miyako city area (data of the Tohoku Earthquake Tsunami Survey Group).

In another case, an additional tsunami source, north of existing source, maybe necessary to explain high inundation in the North Sanriku Coast. We should notice that existing source is traced by the 1st day aftershock distribution and can not be extended to the north. Additional tsunami source may have different nature, submarine landslide for example.

The two-stage tsunami waveforms, having gradual rise and impulsive high amplitude wave were well reproduced with a single plane source model due to localization of tsunami source near the eastern shallow edge of fault plane. This effect of our single plane model may mimic similar effect of the back-stop fault of the real fault model in Japan Trench (Tsuji et al. 2011), or effect of an additional uplift of sediments near a toe of an inner trench slope due to a large horizontal slip (Tanioka and Seno, 2011, Gusman *et al*., 2011). 3D curved fault model may be necessary for accurate source modeling and tsunami simulation. For example, inconsistency of simulated narrow peaks with observed wide peaks in the southern part of the model (gauges 801, 803) may be related to this inaccuracy of the fault surface modeling.

AKCNOWLEDGEMENT

We used the tsunami waveform data of the Nationwide Ocean Wave Information network for Ports and Harbours (NOWPHAS), and tsunami field observations of the Joint Tohoku Earthquake Tsunami Survey Group. Bathymetry and topography models are provided by JODC, JAMSTEC, JHA and GSI. We are indebt to James Kirby, Philip Watts and Stéphan Grilli, provided tsunami simulation program. This study was supported by the Japan Nuclear Energy Safety Organization (JNES)

REFERENCES

Bouchon, M. (1981). A simple method to calculate Green's functions for elastic layered media *Bull. Seismol. Soc. Am.* **71**, 959-971.

Gusman, A.R., Tanioka, Y., Sakai S. and Tsushima, H. (2011). Source model of the 2011 Tohoku tsunami estimated from tsunami waveforms and crustal deformation data *EPSL*, submitted.

Hayashi, Y., Tsushima, H., Hirata, K., Kimura, K. and Maeda, K. (2011). Tsunami source area of the 2011 off the Pacific Coast of Tohoku Earthquake determined from tsunami arrival times at offshore observation stations *Earth Planets Space* **63:7**, 809-813.

Hayes, G.P. (2011). Rapid Source Characterization of the 03--11—2011 Mw 9.0 Off the Pacific Coast of Tohoku Earthquake *Earth Planets Space* **63:7**, 529-534.

Ide, S., Baltay, A. and Beroza, G. (2011). Shallow dynamic overshoot and energetic deep rupture in the 2011 *M*w 9.0 Tohoku-oki earthquake *Science*, doi:10.1126/science.1207020.

Ioualalen, M., Pelletier, B., Regnier, M. and Watts, P. (2006). Numerical modeling of the 26th November 1999 Vanuatu tsunami *J. Geophys. Res.* **111**, C06030, doi:10.1029/2005JC003249.

Irikura, K. and Miyake, H. (2010). Recipe for Predicting Strong Ground Motion from Crustal Earthquake Scenarios *Pure Appl. Geophys.* **168:1-2**, 85-104.

Ito, T., Ozawa, K., Watanabe, T. and Sagiya, T. (2011). Slip distribution of the 2011 Tohoku earthquake inferred from geodetic data *Earth Planets Space* **63:7**, 627-630.

Kennet, B.L.N. and Kerry, N.J. (1979). Seismic waves in a stratified half space *Geophys. J. R. Astr. Soc.* **57**, 557-583.

Kurahashi, S. and Irikura, K. (2011). Source model for generating strong ground motions during the 11 March 2011 off the Pacific Coast of Tohoku Earthquake *Earth Planets Space* **63:7**, 571-576.

Lay, T., Ammon, C. J., Kanamori, H., Lian Xue and Kim, M.J. (2011). Possible large near-trench slip during the great 2011 Tohoku (*M*w 9.0) Earthquake *Earth Planets Space* **63:7**, 687-692.

Murotani, S., Miyake, H. and Koketsu, K. (2008). Scaling of characterized slip models for plate-boundary earthquakes *Earth Planets Space* **60**, 987–991.

Okada, S. (1985). Surface displacement due to shear and tensile faults in a half-space *Bull. Seismol. Soc. Am.* **75**, 1135–1154.

Satake, K., Sakai, S., Fujii, Y., Shinohara, M. and Kanazawa, T. (2011). Tsunami Source of 2011 Tohoku Earthquake *Kagaku* **81**, 407-410.

Somerville, P., Irikura, K., Graves, R., Sawada, S., Wald, D., Abrahamson, N., Iwasaki, Y., Kagawa, T., Smith, N. and Kowada, A. (1999). Characterizing earthquake slip models for the prediction of strong ground motion *Seismol. Res. Lett.* **70**, 59–80.

Tanioka, Yu. and Seno, T. (2001). Sediment effect on tsunami generation of the 1896 Sanriku tsunami earthquake *Geophys. Res Lett.* **28:17**, 3389-3392.

Tsuji, T., Ito, Yo., Kido, M., Osada, Yu., Fujimoto, H., Ashi, J., Kinoshita, M. and Matsuoka, T. (2011). Potential tsunamigenic faults of the 2011 off the Pacific coast of Tohoku Earthquake *Earth Planets Space* **63:7**, 831–834.

Watts, P., Grilli, S.T., Kirby, J.T., Fryer, G.J. and Tappin, D.R. (2003). Landslide tsunami case studies using a Boussinesq model and a fully nonlinear tsunami generation model. *Nat. Hazards and Earth Sci. Systems, EGU*, **3:5**, 391-402.

Wei, G. and Kirby, J.T. (1995). A time-dependent numerical code for extended Boussinesq equations. *J. Waterw. Port Coastal Oceanic Eng.* **121**, 251– 261.

Yoshida, K., Miyakoshi, K. and Irikura, K. (2011). Source Process of the 2011 Off the Pacific Coast of Tohoku Earthquake Inferred from Waveform Inversion with Long-Period Strong-Motion Records. *Earth Planets Space* **63:7**, 577-582.